

Microstructure, hardness and tensile properties of fusion zone in laser welding of advanced high strength steels

A. Santillan Esquivel^{1,2}, S. S. Nayak¹, M. S. Xia^{1,3} and Y. Zhou^{*1}

Fusion zone (FZ) of advanced high strength steel welds, with similar and dissimilar combinations, in diode laser welding was characterised in respect to microstructure, microhardness and tensile strength. Average FZ hardness and tensile properties were correlated to the respective microstructure and chemistry. A linear relationship of the FZ hardness with carbon content was observed for all welding combinations; however, carbon equivalent representing all the alloying elements in the FZ showed slightly better linear fit. The plot of calculated martensite hardness and experimental FZ hardness versus carbon content represented three regions: high carbon content, >0.15 wt-%, leads to fully martensitic microstructure with good hardness matching; reducing the carbon content to 0.1–0.15 wt-% resulted in mixed microstructure consisting dominantly martensite with few fraction of ferrite giving hardness value just below martensite hardness; and for low carbon content the microstructure was dominantly soft ferrite phase causing large deviation from martensite hardness. Fusion zone tensile strength was observed to follow linear relationship with hardness.

On a caractérisé la zone de fusion (FZ) de soudage au laser à diodes de soudures avancées d'acier à forte résistance, avec combinaisons similaires et dissimilaires, par rapport à la microstructure, à la microdureté et à la résistance mécanique. On a corrélé les propriétés moyennes de dureté et de traction de la FZ à leur microstructure et à leur chimie respective. On a observé une relation linéaire de la dureté de la FZ avec la teneur en carbone pour toutes les combinaisons de soudage; cependant, l'équivalent en carbone représentant tous les éléments d'alliage de la FZ montrait un ajustement linéaire légèrement meilleur. La courbe de la dureté calculée de la martensite et de la dureté expérimentale de la FZ par rapport à la teneur en carbone représentait trois régions: une teneur élevée en carbone, > 0.15 wt-% en poids, conduisait à une microstructure entièrement martensitique avec bonne corrélation de la dureté une réduction de la teneur en carbone à 0.1–0.15 wt-% en poids avait pour résultat une microstructure mixte consistant principalement de martensite avec quelques fractions de ferrite, donnant une valeur de dureté juste au-dessous de la dureté de la martensite; et pour une faible teneur en carbone, la microstructure était principalement une phase de ferrite molle produisant une grande déviation par rapport à la dureté de la martensite. On a observé que la résistance à la traction de la zone de fusion suivait une relation linéaire avec la dureté.

Keywords: Advanced high strength steel, Laser welding, Microstructure, Hardness, Tensile strength

This paper is part of a special issue on Advances in High Temperature Joining of Materials

Introduction

Advanced high strength steels (AHSSs) have received high attention due to the continuing need for vehicle weight reduction and improved safety due to their high strength and ductility. Different AHSSs are developed by employing unique processing routes and alloying additions leading to typical microstructure and

¹Center for Advanced Materials Joining, Mechanical and Mechatronics Engineering, University of Waterloo, Waterloo, ON N2L 3G1, Canada

²CORPORACIÓN MEXICANA DE INVESTIGACION EN MATERIALES, S.A. DE C.V. (COMIMSA), Science and Technology No. 790 Col. Saltillo 400, CP 25290 Saltillo, Coahuila, Mexico

³Central Iron & Steel Research Institute, No. 76, Xueyuan Nan Lu, Beijing 100081, China

*Corresponding author, email nzhou@uwaterloo.ca

mechanical properties. Advanced high strength steel is commonly referred to dual phase (DP), transformation induced plasticity (TRIP), complex phase (CP) and martensitic steels which are characterised as steels with a yield strength >300 MPa and a tensile strength >600 MPa.^{1,2} In the context of microstructure, DP steel consists of ferrite matrix embedded with martensite islands whereas TRIP steel microstructure is similar to DP steel with additional presence of retained austenite. In addition, DP and TRIP steels may contain few bainite regions depending on the alloying elements in them. Apart from AHSS, high strength low alloy (HSLA) steels are also popular in autobody designing, which having tensile strength <500 MPa is classified as conventional high strength steel. Dual phase and TRIP steels are known to have a greater ratio of tensile strength over yield strength than conventional HSLA steel. Additionally, the higher work hardening behaviour of AHSS correlates to better formability and crash performance of automotive components.³ Furthermore, the relative amounts of ferrite and martensite phases can be adjusted through intercritical annealing treatment even with the same steel chemistry.^{1,2}

In literatures, there are many reports on the welding of HSLA steels.^{4,5} However, the weldability of AHSS is not yet fully understood. In literatures, it has been reported that AHSS can be welded with all conventional welding methods currently used in the automotive industry, such as resistance spot welding,⁶⁻⁸ gas metal arc welding⁹ and laser welding.¹⁰⁻¹³ In resistance spot welding, the contact between electrode tips and sheet metal will result in the deterioration of the tips and lap welding is necessary. In arc welding, the weld possesses a wider heat affected zone due to its lower power density. On the other hand, in automotive manufacturing a wide use of different AHSS sheets is involved in which laser welding is taking a great relevance for welding tailored blanks, of both similar and dissimilar steel combinations, for formed panels. This helps in achieving environmental goals, improved vehicle response, and increased passenger safety through vehicle light weighting by compounded reduction in body weight. In this regard, several studies have been focused on laser welding of AHSS, such as microstructure and mechanical properties,^{10,12-14} evaluation of performance by formability testing^{15,16} and fatigue behaviour.^{14,17} In the current literatures, however, there are no reports accounting the study on correlation of fusion zone (FZ) microstructure and its properties in laser welded AHSS, mainly in dissimilar welds.

In this study, HSLA, DP600, DP780, DP980 and TRIP780 steel sheets were welded by laser welding, in both similar and dissimilar combinations with the objective for comparing microstructure, hardness and tensile strength of the FZ. In addition, the FZ hardness and strength were correlated to the carbon content and chemistry, i.e. carbon equivalent CE_Y .

Experimental

The starting materials in this study were four zinc coated AHSS sheets namely DP600, DP780, DP980 and TRIP780 sheets. High strength low alloy steel sheet was also selected as a benchmark and representative conventional high strength steel. The chemistries of these steels along with thickness, coating type and carbon equivalent are enlisted in Table 1. Carbon equivalent was calculated using Yurioka's formula¹⁸ given by equation (1) involving all the alloying elements so as to represent the bulk chemistry of the AHSS

$$CE_Y = C + f(C) \left[\frac{Si}{24} + \frac{Mn}{6} + \frac{Cu}{15} + \frac{Ni}{20} + \frac{(Cr + Mo + Nb + V)}{5} \right] \quad (1)$$

where

$$f(C) = 0.75 + 0.25 \tanh [20(C - 0.12)]$$

In the case of dissimilar combination, the carbon content, chemistry and CE_Y were calculated by taking average of the respective values of the employed steels. The details of the dissimilar weld analysed in the present study are listed in Table 2.

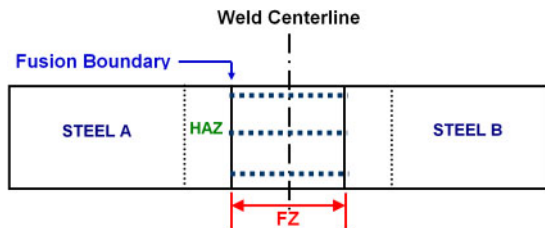
A Nuvonyx ISL-4000L 4 kW diode laser and Panasonic 6-axis robotic arm with 805 nm wavelength generating a rectangular beam of 12 x 0.9 mm was used for performing the laser welding experiments. The welding conditions for the experiments are shown in Table 3. Rectangular steel sheets of dimensions

Table 2 Dissimilar laser welding combinations studied and calculated chemistry (wt-%) and carbon equivalent (CE_Y) of respective FZ

Weld combinations	C	Mn	Si	Cr	CE_Y
HSLA-DP600	0.103	1.035	0.284	0.031	0.233
HSLA-DP780	0.087	1.35	0.132	0.141	0.283
HSLA-TRIP780	0.126	1.13	0.926	0.032	0.333
DP600-TRIP780	0.166	1.541	1.008	0.0215	0.427
DP780-TRIP780	0.149	1.855	0.856	0.132	0.477

Table 1 Chemistry (wt-%), thickness, coating type and hardness of different steels investigated in present study

Steel (coating type)	HSLA (GI)	DP600 (GI)	DP780 (GA)	DP980 (GA)	TRIP780 (GI)
C	0.063	0.144	0.111	0.132	0.188
Mn	0.62	1.45	2.08	1.907	1.631
Si	0.233	0.334	0.031	0.032	1.618
Cr	0.041	0.020	0.241	0.161	0.023
CE_Y	0.139	0.326	0.427	0.475	0.527
Hardness/HV	167	175	250	301	265
Thickness/mm	1.00	1.20	1.15	1.20	1.00



1 Schematic illustration of different weld zones developed in laser welding of two dissimilar steels A and B: hardness indentation lines were marked by blue dotted lines within FZ

50 × 100 mm were used which were cleaned by acetone before welding to avoid oxidation and impurities. Laser welding was carried out at a speed of 1.0 m min⁻¹ under argon shielding gas, with a flowrate of 30 L min⁻¹. It is to be noted that all the welds were fully penetrated and no weld defects were detected. Total 10 welds, five each of similar (Table 1) and dissimilar combination (Table 2), were prepared from the five selected steels.

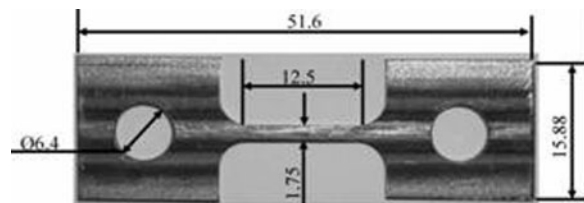
Welded samples were sectioned using an abrasive disc cutter, hot mounted using bakelite powder followed by grinding and polishing down to 1 μm using conventional metallographic procedures. For microstructural characterisation the mirror polished mounted specimens were etched with 1% nital solution. Microstructure of the weldments was characterised using an Olympus BX51M light optical microscope and a JEOL JSM 6460 scanning electron microscope respectively.

Hardness was measured using a LECO Vickers microhardness tester along three lines within the FZ using 200 g load and 15 s dwelling time. One line of indentation was made each on top and bottom side of the FZ whereas a third line was run at the centre. Figure 1 shows the schematic illustration of the hardness measurements within the FZ. To avoid contributions from the neighbouring indents, indentations were separated by 200 μm and the lines of indentation were separated by 500 μm. Average of the measurements from the three lines of indentations is reported as hardness of the FZ. A specially designed miniature tensile specimens excluding the HAZ and base metal in the gauge were used for tensile testing; the specimen dimensions, in mm, are shown in Fig. 2. To evaluate the tensile properties of the FZ, tensile testing was carried out at room temperature with a strain rate of 1 × 10⁻³. A minimum of three coupons were tested for each combination and the average readings are reported with standard deviation representing the error bars.

Results and discussion

Microstructure and hardness of FZ

Hardness profiles of the welds of three typical steels and corresponding FZ microstructure are illustrated in



2 Illustration of typical coupon used for evaluating tensile properties of FZ: all dimensions are in mm

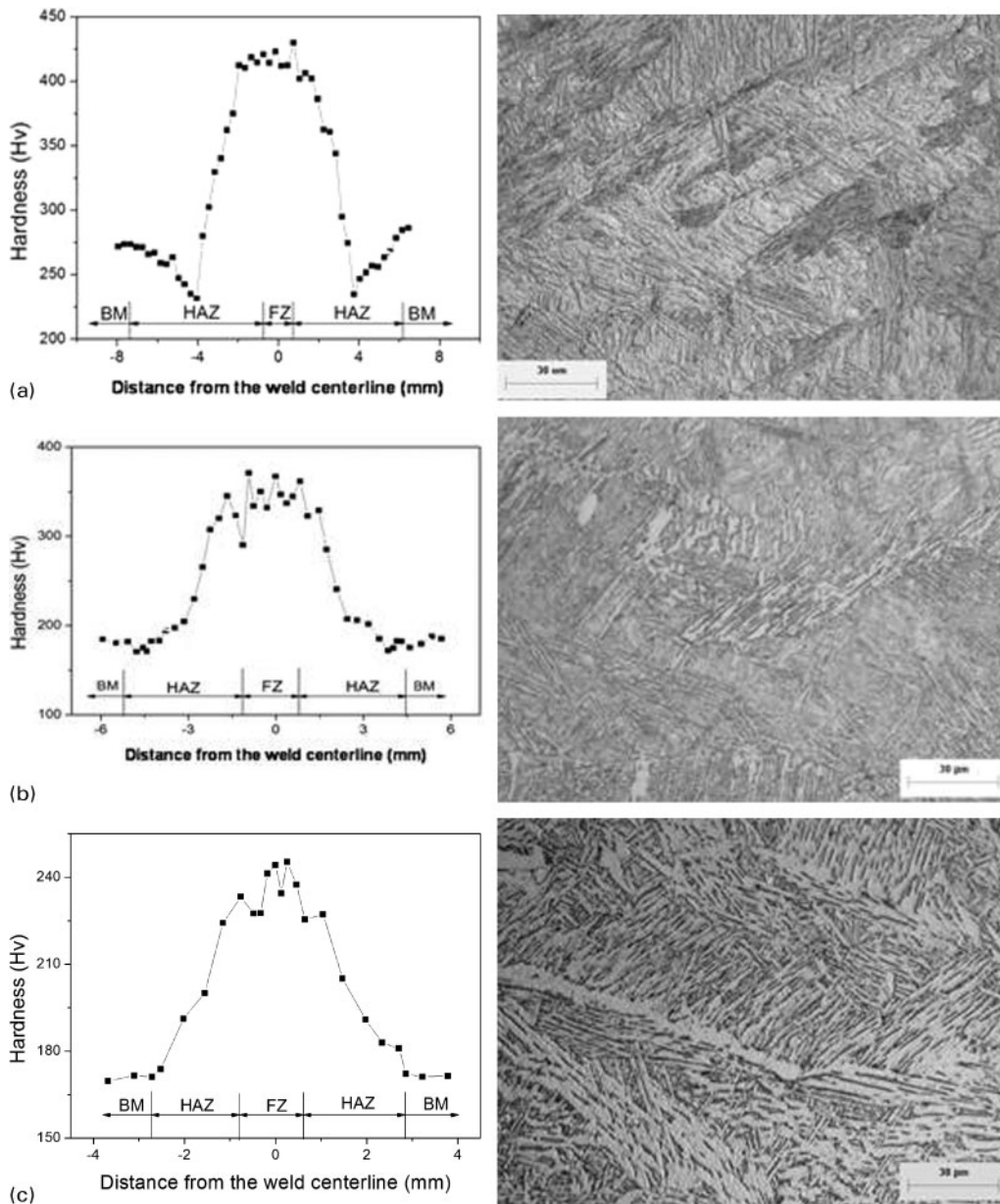
Fig. 3. It can be found that the hardness profile was relatively flat across the FZ in all the cases. Hardness valleys were also seen in the outer part of the HAZ of DP steels (Fig. 3a and b), in which the hardness locally dropped below the base metal hardness. Such valley is termed as HAZ softening which has previously been observed in outer HAZ of DP steels welded by various welding techniques and was attributed to local tempering, by the weld thermal cycle, of the martensite phase present in the base metal. The detail examination of HAZ softening is reported elsewhere.^{19–25}

Like similar weld combinations, all the dissimilar weld combinations studied in the present work formed FZ with uniform microstructure throughout concluding homogeneity in the chemistry during laser welding. For example, hardness profiles taken at three different lines within the FZ of DP600–HSLA weld combination were very consistent (Fig. 4) indicating a homogeneous microstructure, which was corroborated well by the micrographs taken from different regions, DP600 side, centre and HSLA side, of the FZ (insets in Fig. 4) illustrating a similar microstructure containing predominantly ferrite phase with few fraction of needle-like martensite. The hardness level within the FZ was in the range of 200–230 HV which is attributed to the lower average carbon content (0.103 wt-%) in the FZ (Table 2). The detailed relation between FZ hardness and carbon content is described in the following paragraph.

Figure 5 shows the FZ hardness as a function of carbon content for data from this work. There were four steels studied in this work with similar and dissimilar combination with a carbon range from 0.06 to 0.188 wt-%. Fusion zone with higher carbon showed higher hardness. Lower carbon content (for example, 0.08 wt-%) in the FZ resulted in the lowest hardness values out of all the FZ tested, ranging 225 ± 13 HV; whereas FZ with a highest carbon content (0.188 wt-%) resulted in the highest hardness value of 465 ± 19 HV as shown in Fig. 5a. Richer chemistry FZ also contains higher concentrations of alloying elements such as Mn, Cr and Si (Tables 1 and 2). The effects of these elements on the FZ hardness are not yet fully understood and further research is required to detail their influence. However, it is reported that the addition of some alloying elements can enhance the

Table 3 Details of diode laser welding parameter used in present study

Speed/m min ⁻¹	Power/kW	Voltage/V	Current/A	Shielding gas (argon)/L min ⁻¹
1	4	40	40	30



a DP980; b DP600; c HSLA

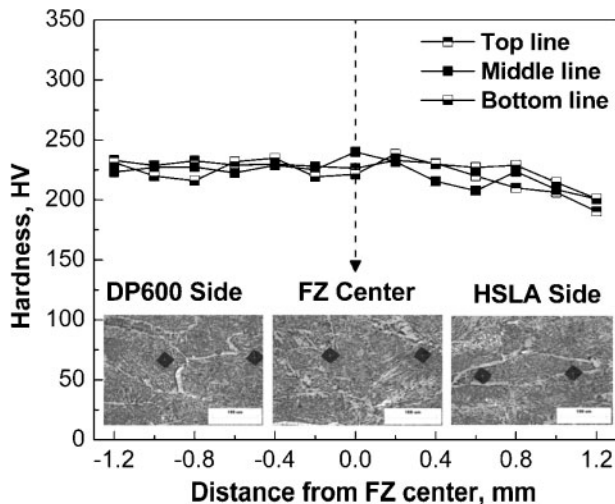
3 Representative hardness profiles of different welds and corresponding FZ microstructure

effectiveness of carbon in martensite.^{26,27} Alloying elements can aid in the formation of martensite by increasing minimum cooling time and by retarding the kinetics of ferrite and bainite formation, and hence the CE_Y is considered as an effective means of the effects that alloying elements have on steel hardenability. Figure 5b shows the variation of FZ hardness as a function of CE_Y . Trends show that FZ hardness increases with richer chemistries that produce higher CE_Y values. It was observed that CE_Y shows that a better linear relationship with regression coefficient of 0.938 was obtained between FZ hardness and CE_Y compared to that with carbon content which gave a linear relationship with a lower regression coefficient of 0.913 (Fig. 5a). Extracting the linear relationship between FZ hardness and CE_Y gives

the following equation:

$$H_{FZ} = 117 + 635CE_Y \tag{2}$$

where H_{FZ} is fusion zone hardness and CE_Y is carbon equivalent calculated using equation (1). The relationship in equation (2) matches closely to the similar relationship obtained in resistance spot welding of AHSS.²⁸ Equation (2) provides an improved method for determining the FZ hardness of various steels. In addition, equation (2) accounts for various alloying elements used in the production of AHSS. Therefore, it was concluded that by using the Yurioka carbon equivalent equation, i.e. equation (1), which includes an accommodation factor for a wide range of chemistries, a



4 Hardness profiles within FZ of dissimilar weld DP600–HSLA and microstructure at three locations: DP600 side, centre and HSLA side of FZ

more reliable relationship between FZ hardness and chemistries can be made, compared to carbon content, for a given laser welding condition.

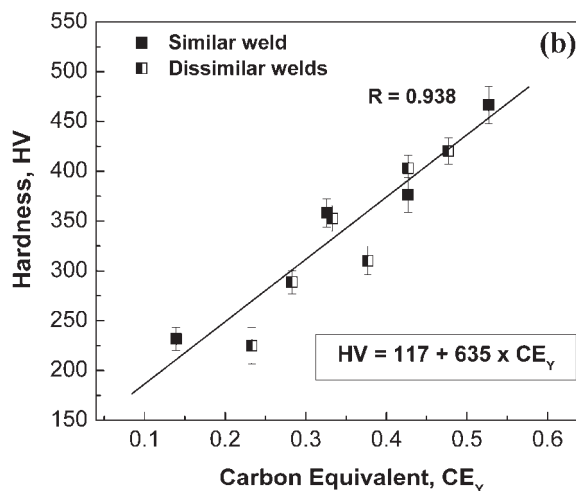
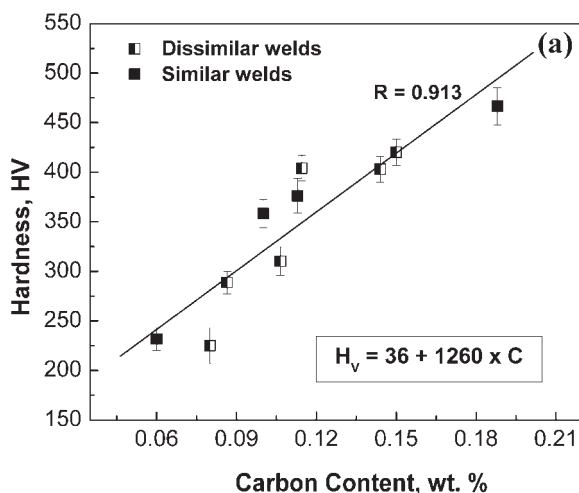
The only reason for the variation of FZ hardness as a function of carbon content shows in Fig. 5a can be due to variation in microstructure, as the welding conditions were kept constant, as illustrated in Figs. 3 and 6. It may be recalled that Fig. 3 indicated that the more rich the steel with carbon, the less the variation and also the higher average FZ hardness. For example, DP980 FZ (Fig. 3a) has higher hardness and little variation compared to that in the case of DP600 (Fig. 3b) and HSLA (Fig. 3c), which have lower hardness and large variation. It means more homogenous microstructure composition was achieved in FZ with richer chemistry. The FZ microstructures, shown in Figs. 3 and 6, indicated a variation which is reflected in the average hardness values (Fig. 5a), concluding that both vary with respect to the carbon level in the FZ. The lowest hardness in the FZ

containing a lower carbon content (0.08 wt-%) was corroborated well by the microstructure which consisted mixture of ferrite phase and martensite islands (Fig. 6a). With increase in carbon content in the FZ resulted in gradual decrease in the soft ferrite phase and increase in the hard martensite phase as shown in Fig. 6 giving a maximum hardness value from the FZ containing a highest carbon content (Fig. 6d) which exhibited values above 466 ± 19 HV (Fig. 5a).

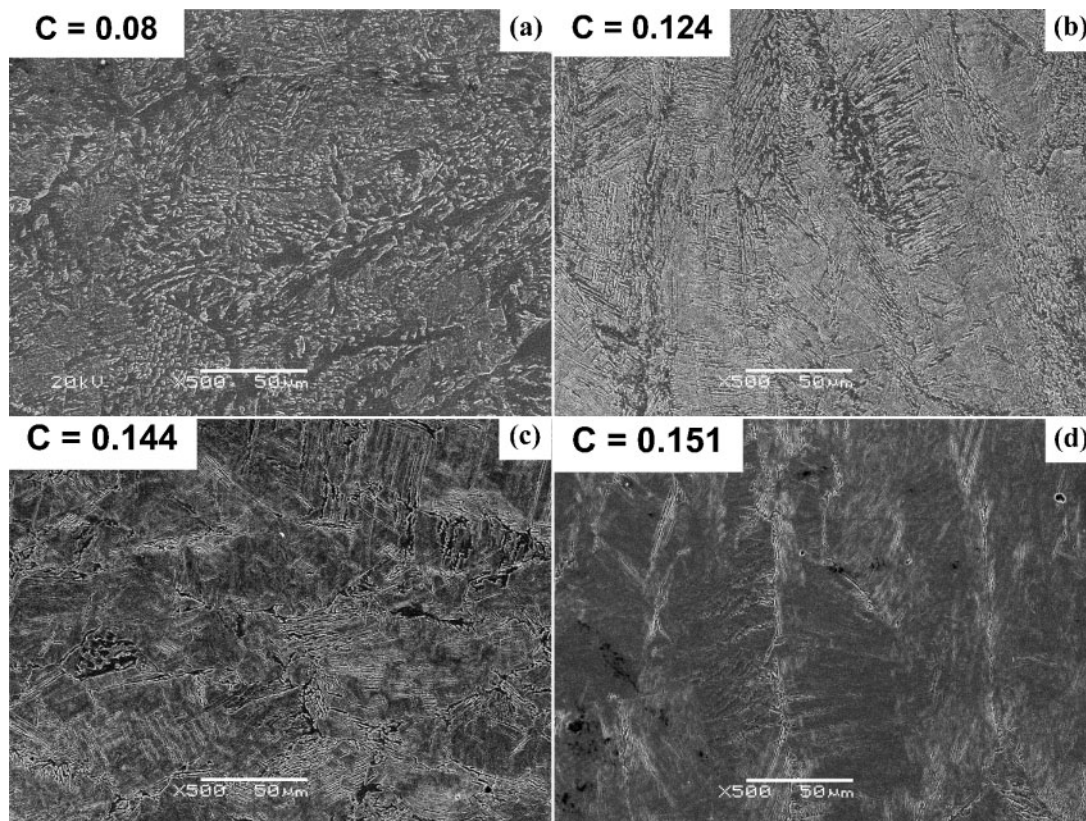
Carbon increases the ability to form martensite, and is also known to increase the hardness of martensite. Using carbon content to predict martensite hardness was feasible for traditional lean chemistry FZ, which mainly contained only iron and carbon and low levels of other alloying elements. Yurioka²⁹ measured fully martensite hardness of various steels produced using high cooling rates achieved in arc welding and derived the following relationship

$$H_M = 884C + 294 \quad (3)$$

where H_M is the martensite hardness and C is the carbon content in it. Figure 7 shows the plot of experimental FZ hardness versus carbon content. Calculated FZ martensite hardness attained from equation (3) is also plotted as the straight line. It can be found that the microstructure in the FZ of these steel is composed from full martensite to the mixture of ferrite and martensite phases, as observed in Fig. 6. The plot shown in Fig. 7 can be divided into three regions. In region I, the experimental hardness value falls in the line of calculated martensite hardness indicating that the FZ should form martensite phase which was confirmed by the microstructure (Fig. 6d). Region II includes FZ with a lower carbon content, resulting decreasing carbon equivalent, which deviated the experimental hardness values from martensite hardness suggesting a microstructure softer than martensite, as indicated by scanning electron micrograph in Fig. 6c showing a mixture of ferrite and martensite phase. Further decrease in carbon content in the FZ, region III, indicated hardness values which deviate largely from the martensite



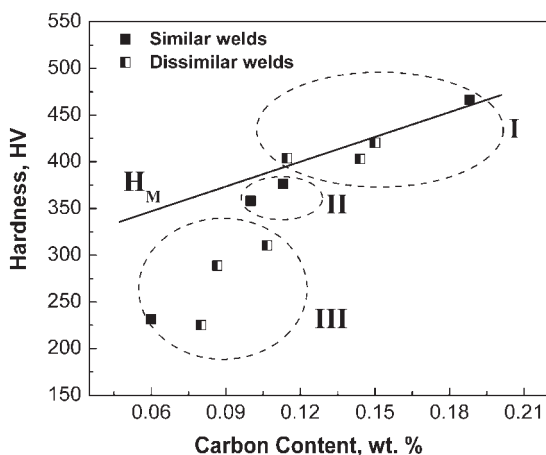
5 Variation of FZ hardness with a carbon content and b carbon equivalent in laser welds with both similar and dissimilar combination: regression formulae obtained using linear fit of experimental data are also included



a HSLA-DP600; b HSLA-TRIP780; c DP600-TRIP780; d DP780-TRIP780

6 Variations in FZ microstructure in laser welds as function of carbon content

hardness confirming formation of microstructure that is not softer than martensite which was confirmed by Fig. 6a. Therefore, it was concluded that the martensite hardness formula given by Yurioka²⁹ can be applied to determine the FZ hardness and the predicting the corresponding microstructure.

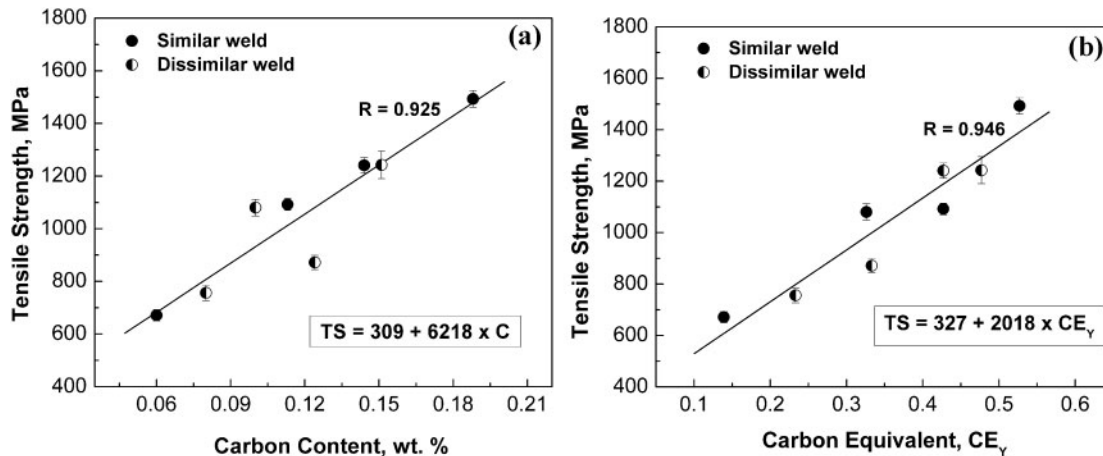


7 Variation of FZ hardness as function of carbon content in AHSS laser welds: calculated martensite hardness H_M using Yurioka formula is also included as straight line to assist in predicting FZ microstructure

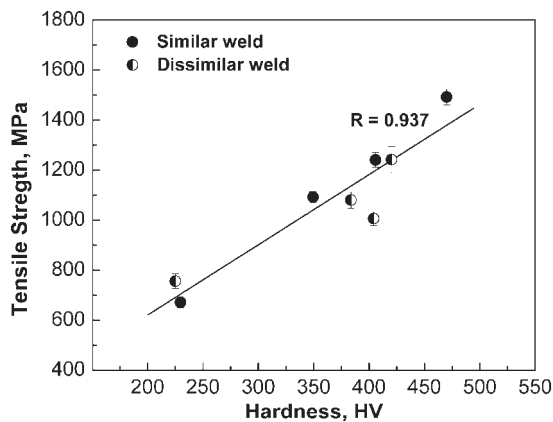
Tensile strength of FZ and its correlation to hardness

Tensile strength of the FZ was observed to have a linear relationship with the carbon content and CE_Y , as shown in Fig. 8. Like FZ hardness, the tensile strength was also found to increase with increase in carbon content and in turn the CE_Y values. The reason for which is also attributed to the microstructure (Figs. 3 and 6) as described in aforementioned paragraphs. For instance, higher carbon containing FZ forms martensite microstructure (Fig. 6d) resulting in higher strength; whereas reducing the carbon content decreases the strength due to formation of microstructure predominantly containing ferrite with few fractions of martensite (Fig. 6a). In a general way, it can be said that increasing the carbon content and the alloying additions the strength of the FZ can be increased linearly.

Hardness value is often treated as the representative of strength of a material. Therefore, the idea of estimating the tensile properties of a material in terms of the yield stress and ultimate tensile stress from the hardness values, rather than the application of tension testing, is popular as a quick method to predict strength.³⁰ In this context, Yurioka and Kojima³¹ reported that the FZ hardness can be correlated with the ultimate tensile strength; however, the work was confined to the arc welding process. In the present work, these two properties of FZ were correlated to each other and a linear equation as follows was



8 Variation of FZ tensile strength as function of a carbon content and b carbon equivalent in laser welds of AHSS: regression formulae obtained using linear fit of data are also included



9 Relationship between tensile strength and hardness of FZ studied in present work

obtained with a very high *R* value (Fig. 9)

$$TS = A \times HV + B \tag{4}$$

where *TS* and *HV* are the ultimate tensile strength in MPa and the hardness values of FZ respectively. The regression coefficient of the linear equation obtained in the present work and those obtained by Yurioka and Kojima³¹ are summarised in Table 4. The coefficients are almost in the same range taking into account of the measurement error. It means that the linear equation above can be used to predict the tensile strength with the knowledge of hardness values of the FZ in AHSS. This equation is also reasonable to adopt as the hardness is

Table 4 Comparison of coefficient for regression formulae in linear relation of tensile strength *TS* in MPa and hardness *HV* of FZ in present study and that reported by Yurioka and Kojima³¹

$TS = A \times HV + B$	A	B
Present study	2.76	21.6
Yurioka	3.0	22.3

regarded as the plastic deformation resistance of a material; therefore, the increase in hardness means the increase in the plastic deformation resistance and in turn the tensile strength.

Conclusions

A linear relationship of the FZ hardness with a carbon content was observed for both all welding combinations; however, carbon equivalent representing all the alloying elements in the FZ has better linear fit when plotted against hardness. The plot of calculated martensite hardness and experimental FZ hardness versus carbon content represented three different regions indicating that the martensite content in the FZ microstructure decreased with decrease in the carbon content and alloying additions. Like hardness, FZ tensile strength followed a linear relationship with carbon content and alloying level *CE_y*. Furthermore, tensile strength (*TS* in MPa) was observed to follow linear relationship with hardness *HV* as given by the formula: $TS = 2.76 \times HV + 21.6$.

Acknowledgements

The financial support from Auto21, one of the Networks of Centres for Excellence supported by the Canadian Government, The Initiative for Automotive Manufacturing Innovation (IAMI) supported by the Ontario Government, International Zinc Association (IZA), Belgium and ArcelorMittal Dofasco in Canada is highly acknowledged. A. Santillan Esquivel gratefully acknowledges the financial support of COMMIMSA, Mexico for carrying out this research in University of Waterloo and his stay in Canada.

References

- H. Bhadeshia and R. Honeycombe: 'Steels: microstructure and properties', 3rd edn; 2006, Butterworth-Heinemann, Oxford.
- B. C. de Cooman: 'Structure-properties relationship in TRIP steels containing carbide-free bainite', *Curr. Opin. Solid State Mater. Sci.*, 2004, **8**, 285–303.

Published by Maney Publishing (c) Canadian Institute of Mining, Metallurgy and Petroleum

3. G. H. Thomas and M. X. Chen: 'Formability performance comparison between dual phase and HSLA steels', *Iron Steelmak. (USA)*, 2002, **29**, 27–32.
4. K. Banerjee and U. K. Chatterjee: 'Effect of microstructure on hydrogen embrittlement of weld-simulated HSLA-80 and HSLA-100 steels', *Metall. Mater. Trans. A*, 2003, **34A**, 1297–1309.
5. S. Dinda, C. Belleau and D. K. Kelley: Int. Conf. on 'Technology and applications of HSLA steels', Philadelphia, PA, USA, October 1984, ASM International, 475–483.
6. M. I. Khan, M. L. Kuntz and Y. Zhou: 'Effect of weld microstructure on the static and impact performance of resistance spot welded (RSW) joints in advanced high strength steels (AHSS)', *Sci. Technol. Weld. J.*, 2008, **13**, 294–304.
7. V. H. Baltazar Hernandez, M. L. Kuntz, M. I. Khan and Y. Zhou: 'Influence of microstructure and weld size on the mechanical behaviour of dissimilar AHSS resistance spot welds', *Sci. Technol. Weld. Join.*, 2008, **13**, 769–776.
8. M. Amrithalingam, M. Hermans and I. Richardson: 'Microstructural development during welding of silicon- and aluminium-based transformation-induced plasticity steel-inclusion and elemental partitioning analysis', *Metall. Mater. Trans. A*, 2009, **40A**, 901–909.
9. T. K. Han, S. S. Park, K. H. Kim, C. Y. Kang, I. S. Woo and J. B. Lee: 'CO₂ laser welding of 800 MPa class TRIP steel', *ISIJ Int.*, 2005, **45**, (1), 60–65.
10. M. Xia, Z. Tian, L. Zhao and Y. N. Zhou: 'Metallurgical and mechanical properties of fusion zones of TRIP steels in laser welding', *ISIJ Int.*, 2008, **48**, 483–488.
11. J. Chen, K. Sand, M. S. Xia, C. Ophus, R. Mohammadi, M. L. Kuntz, Y. Zhou and D. Mitlin: 'TEM and nanoindentation study of the weld zone microstructure of a diode laser joined automotive TRIP steel', *Metall. Mater. Trans. A*, 2008, **A39**, 593–603.
12. R. S. Sharma and P. Molian: 'Yb:YAG laser welding of TRIP780 steel with dual phase and mild steels for use in tailor welded blanks', *Mater. Des.*, 2009, **30**, 4146–4155.
13. M. Xia, Z. Tian, L. Zhao and Y. N. Zhou: 'Fusion zone microstructure evolution of Al-alloyed TRIP steel in diode laser welding', *Mater. Trans. JIM*, 2008, **49**, 746–753.
14. N. Farabi, D. L. Chen and Y. Zhou: 'Microstructure and mechanical properties of laser welded dissimilar DP600/DP980 dual-phase steel joints', *J. Alloys Compd*, 2011, **509**, (3), 982–989.
15. H. Shao, J. Gould and C. Albright: 'Laser blank welding high-strength steels', *Metall. Mater. Trans.*, 2007, **38**, 321–331.
16. S. K. Panda, J. Li, V. H. Baltazar Hernandez, Y. Zhou and F. Goodwin: 'Effect of weld location, orientation and strain path on forming behavior of AHSS tailor welded blanks', *Trans. ASME: J. Eng. Mater. Technol.*, 2010, **132**, (10), 041003–1–11.
17. N. Farabi, D. L. Chen, J. Li, Y. Zhou and S. J. Dong: 'Microstructure and mechanical properties of laser welded DP600 steel joints', *Mater. Sci. Eng. A*, 2010, **A527**, 1215–1222.
18. N. Yurioka and T. Kasuya: 'A chart method to determine necessary preheat in steel welding', *Weld. World*, 1995, **35**, 327–334.
19. C. Hsu, P. Soltis, M. Carroscia, D. Barton and C. Occhialini: 'Weldability of dual-phase steel with arc welding processes', Proc. 11th Sheet Metal Welding Conf., Sterling Heights, MI, USA, May 2004, AWS, 1–11.
20. M. Xia, E. Biro, Z. Tian and Y. N. Zhou: 'Effects of heat input and martensite on HAZ softening in laser welding of dual phase steels', *ISIJ Int.*, 2008, **48**, 809–814.
21. V. H. Baltazar Hernandez, S. K. Panda, Y. Okita and Y. Zhou: 'A study on heat affected zone softening in resistance spot welded dual phase steel by nanoindentation', *J. Mater. Sci.*, 2010, **45**, 1638–1647.
22. E. Biro, J. R. McDermid, J. D. Embury and Y. Zhou: 'Softening kinetics in the subcritical heat-affected zone of dual-phase steel welds', *Metall. Mater. Trans. A*, 2010, **41A**, 2348–2356.
23. S. S. Nayak, V. H. Baltazar Hernandez and Y. Zhou: 'Effect of chemistry on nonisothermal tempering and softening of dual-phase steels', *Metall. Mater. Trans. A*, 2011, **42A**, 3242–3248.
24. Y. Okita, V. H. Baltazar Hernandez, S. S. Nayak and Y. Zhou: 'Effect of HAZ-softening on failure mode of resistance spot-welded dual-phase steel', Proc. 14th Sheet Metal Welding Conf., Livonia, MI, USA, May 2010, AWS, 1–12.
25. V. H. Baltazar Hernandez, S. S. Nayak and Y. Zhou: 'Tempering of martensite in dual-phase steels and its effects on softening behavior', *Metall. Mater. Trans. A*, 2011, **42A**, 3115–3129.
26. M. D. Perkas: 'High strength maraging steels', *Met. Sci. Heat Treat.*, 1968, **6**, 415–425.
27. H. Cerjak: 'Mathematical modelling of weld phenomena', Vol. 3; 1997, London, Maney Publishing.
28. M. I. Khan, M. L. Kuntz, E. Biro and Y. Zhou: 'Microstructure and mechanical properties of resistance spot welded advanced high strength steels', *Mater. Trans.*, 2008, **49**, 1629–1637.
29. N. Yurioka: 'Weldability calculations', <http://homepage3.nifty.com/yurioka/exp.html>, (accessed 13 September 2011).
30. S. C. Chang, M. T. Jahn, C. M. Wan, J. Y. M. Lee and T. K. Hsu: 'The determination of Tensile Properties from Hardness Measurements for Al-Zn-Mg Alloys', *J. Mater. Sci.*, 1976, **11**, 623–660.
31. N. Yurioka and K. Kojima: 'A predictive formula of weld metal tensile strength', *Q. J. JWS*, 2004, **22**, 53–60.